Published in final edited form as:
Inorg Chem. 2011 March 7; 50(5): 1648–1655. doi:10.1021/ic101856d.

Europium(III) DOTA-derivatives having ketone donor pendant arms display dramatically slower water exchange

Kayla N. Green, **Subha Viswanathan**, **Federico A. Rojas-Quijano**, **Zoltan Kovacs**, and **A. Dean Sherry***
Advanced Imaging Research Center, UT Southwestern Medical Center, 5323 Harry Hines Boulevard, Dallas, Texas 75390 and Department of Chemistry, University of Texas at Dallas, 800 West Campbell Road, Richardson, Texas 75080.

Abstract

A series of new 1,4,7,10-tetraazacyclododecane-derivatives having a combination of amide and ketone donor groups as side-arms were prepared and their complexes with europium(III) studied in detail by high resolution NMR spectroscopy. The chemical shift of the Eu^{3+}-bound water resonance, the chemical exchange saturation transfer (CEST) characteristics of the complexes, and the bound water residence lifetimes (τ_m) were found to vary dramatically with the chemical structure of the side-arms. Substitution of ketone oxygen donor atoms for amide oxygen donor atoms resulted in an increase in residence water lifetimes (τ_m) and a decrease in chemical shift of the Eu^{3+}-bound water molecule ($\Delta\omega$). These experimental results along with density functional theory (DFT) calculations demonstrate that introduction of weakly donating oxygen atoms in these complexes results in a much weaker ligand field, more positive charge on the Eu^{3+} ion and an increased water residence lifetime as expected for a dissociative mechanism. These results provide new insights into the design of paramagnetic CEST agents with even slower water exchange kinetics that will make them more efficient for *in vivo* imaging applications.

Keywords

PARACEST; MRI; europium; dicarbonyl; water exchange

INTRODUCTION

Paramagnetic lanthanide compounds have had a substantial impact in NMR and magnetic resonance imaging (MRI) since the early 1970's. Gadolinium(Gd^{3+})-based T_1 agents have served as the gold standard for MRI contrast agents since the late 1980's and new directions for Gd^{3+} contrast agents continue to be an active area of research.1⁻4 A variety of molecular designs have been reported as "responsive" Gd^{3+} contrast agents,5 most based on changes in relaxivity that reflect either a change in *q* (number of inner-sphere water molecules) or τ_R (molecular rotation). Although it has proven relatively easy to detect changes in T_1 relaxation in response to biological events *in vitro*, it is more problematical *in vivo* because these complexes are never completely "silent" even if water has no direct access to the Gd^{3+} coordination sphere. This makes it problematical to distinguish between a change in relaxivity *versus* a change in concentration. Consequently, other approaches for introducing

Address for correspondence: Dr. A Dean Sherry, 5323 Harry Hines Boulevard, Dallas, Texas 75390. Tel: +1 214-645-2755. Fax: +1 214-645-2744.

Supporting Information Available: Synthetic procedures for the ligands, ^{13}C NMR spectrum of ligands **1** and **2**, 2D-EXSY spectrum of Eu(**5**), CEST spectra of Eu(**3**)–Eu(**10**). This material is available free of charge via the Internet at http://pubs.acs.org

contrast in MR images are being explored. One relatively promising technique is based on chemical exchange saturation transfer (CEST) principles.6 This technique relies on the selective saturation of a small pool (A) of protons that are in exchange with the much larger bulk water pool (B). Exchange of saturated spins from pool A into B results in a decrease in the intensity of the bulk water spins because they become partially saturated as a result of the exchange. CEST requires slow-to-intermediate exchange between the two pools so by definition this depends upon the frequency difference between the two proton pools, $\Delta\omega$. Slow-to-intermediate exchange requires the condition, $\Delta\omega\tau_m > 1$, where τ_m is the metal bound water residence lifetime. Large $\Delta\omega$ values are advantageous for two reasons; first, a large $\Delta\omega$ makes it easier to selectively saturate at one site without inadvertently partially saturating the other and a large $\Delta\omega$ allows faster exchanging systems to be used for CEST while maintaining the slow-to-intermediate requirement. The effectiveness of CEST agents is also dependent on the number of exchangeable sites (*N*) contained within the CEST agent. The value of *N* is directly related to the sensitivity of the agent while τ_m is a measure of the efficiency of exchange between the pools. Diamagnetic CEST agents such barbituric acid, peptides or nucleic acids have relatively small $\Delta\omega$ values, typically < 5 ppm, so proton exchange must be quite slow to meet the CEST requirement.7 Complexes of paramagnetic Ln(III) ions such as Eu(III), Tb(III), Tm(III) induce large hyperfine shifts in most protons in a complex including any exchangeable NH and OH protons on the ligand arms and any bound water protons. The Ln(III)-bound water protons usually experience much larger hyperfine shifts than the ligand protons in all DOTA-like structures so these are particularly attractive for initiating CEST contrast. However, bound water lifetimes in these complexes can be too short for efficient CEST so it is important to be able to manipulate water exchange using simple chemical principles. Eu(III) complexes with a variety of DOTA-tetraamides typically have sufficiently slow water exchange rates (τ_m on the order of μs) to satisfy the $\Delta\omega > k_{ex}$ exchange requirement so these have been the most widely studied systems to date. In this study, we explored other types of ligand side-chains that can potentially offer a wider range of water exchange kinetics.

Lanthanide ions other than Eu(III) have also shown promise but Eu(III) remains an area of piqued interest since these complexes typically display the longest bound water lifetimes.6 Intrinsically, the bound water lifetime τ_m is directly dependent on the electron deficiency at the lanthanide ion. Qualitatively, the greater the positive character remaining on the Ln^{3+}, the stronger the resulting Ln^{3+}-OH_2 interaction will be. A negatively charged carboxylate group is electron rich and interacts more strongly with Ln^{3+} ions than an oxygen donor atom in the electron deficient amide. A comparison of resident water lifetime for the two Gd^{3+} complexes in Chart 1 clearly illustrates this effect: $GdDOTA^{-}$ (τ_m = 208 ns) vs. $GdDOTA(GlyOEt)_4^{3+}$ (τ_m = 190 μs),8–10 about 3 orders of magnitude different. Therefore, poor donors that leave the central lanthanide ion electron deficient are likely to produce slower water exchange systems (longer τ_m). There are many other factors that affect τ_m including the coordination geometry of the complex (the SAP/TSAP ratio), steric constraints (bulkiness of side-chains) and hydrophobic/hydrophilic effects that alter second coordination sphere water molecules. In a recent paper, we have shown that Eu(III) complexes of DOTA tetraamide ligands with different amino acid extended side-chains produce remarkably different CEST effects.11 Preliminary DFT studies corroborated the relationship between weaker donors and longer τ_m. Morrow and co-workers extended this theory to pendent alcohols, known to remain protonated upon binding to a lanthanide ion.12 Unfortunately, these systems display small $\Delta\omega$ values and have been limited to CH_3CN for observable PARACEST due to shorter than optimal metal bound water lifetime.

β-Diketones are common ligands for lanthanides and lanthanide β-diketonate complexes have found important practical applications ranging from NMR shift reagents to luminescent probes to components in optical devices.13–15 In spite of this, a simple carbonyl oxygen as

a donor atom for Ln^{3+} ions has not been widely used in polyamine-based ligands. Thus, as a part of our research to explore novel ligands for PARACEST agents, we set out to design, synthesize and study cyclen (1,4,7,10-tetraazacyclododecane) derivatives with ketone pendant arms and their complexes with Eu^{3+}. The PARACEST properties of these complexes are the major focus of the work described in this paper.

Experimental Section

General Remarks

All solvents and reagents were purchased from commercial sources and used as received unless otherwise stated. ^{1}H, ^{13}C NMR and CEST spectra were recorded on a VNMRS 400 MHz direct drive Varian console. MALDI mass spectra were acquired on an Applied Biosystems Voyager-6115 mass spectrometer. Metal analysis (ICP-MS, Galbraith) was obtained to calculate metal content in solution before using the metal complexes for CEST experiments.

Fitting of CEST spectra

Numerical solutions to the Bloch equations modified for exchange were obtained by use of a non-linear fitting algorithm in MATLAB. Experimental CEST spectra measured using multiple B_1 powers were fit independently to obtain estimates of the water exchange rates.[6,16]

DFT Studies

Gas phase DFT calculations were performed using a hybrid functional (B3LYP) as implemented in Gaussian 03. For ligands **4**–**6** (see Chart 2) all atoms were optimized using the 6–311G(d,p) basis set, while 3–21G was used for the corresponding metal ion-based calculations. A frequency calculation of each showed the there were no imaginary frequencies, supporting a stable ground state. The .chk files of the optimized geometries were used to produce the Electrostatic Potential Plots and HOMO/LUMO orbital overlays in GaussView.[17–21]

General procedure for the synthesis of the Eu^{3+} complexes

A solution of europium triflate in acetonitrile (about 100 mg in 5 mL) was added to a solution of ligands **1** through **8** (up to 5% excess, to ensure that no free metal is present) in acetonitrile (5 mL). Each reaction was stirred at room temperature for 3 days before the solvent was removed under reduced pressure. Each residue was then dried under high vacuum to constant mass to afford the complex in quantitative yield. The complexes were judged over 95% pure by NMR and MS.

Eu(1)—^{1}H NMR (400 MHz, CD_3CN) δ 13.2 (2H), 7.5(4H), 3.9(4H), 3.6(4H), 3.2 to −0.98(12H), −5.7(4H), −8.8(4H), −12.1(4H); m/z (ESI-MS, ESI^+) 858.75 (100%, $[M^+OH_2]^{3+}$), Calcd. 856.29.

Eu(3)—^{1}H NMR (400 MHz, CD_3CN) δ 23.4(2H), 3.96(18H), 2.41(18H), 1.98(4H), 1.39 to −0.95(16H), −3.10(4H), −4.35(4H), −8.78(4H), −12.2(4H); MALDI+: m/z 1010.72 (100%) $[M+H]^+$, Calcd. 1009.45.

Eu(4)—^{1}H NMR (400 MHz, CD_3CN) δ 13.2(2H), 7.21(4H), 3.84(4H), 3.53(12H), 2.77(9H), 2.54(8H), 1.93 to −1.21(18H), −5.54(4H), 7.49(4H), 12.1(4H); m/z (ESMS, ESI^+) 984.24 (100%, $[M+OH_2]^{3+}$), Calcd. 984.42.

Eu(5)—^{1}H NMR (400 MHz, CD_3CN) δ 35.7(2H), 21.1(4H), 19.9(4H), 15.69(4H), 14.73(4H), 9.40(12H), 7.21(12H), 6.45(9H), 3.45(4H), 3.24(4H), 2.47(4H), 2.37(6H), 1.78 to −1.45(24H), −2.96(4H), −3.37(4H), −5.62(4H), −9.19(4H), −13.02(4H), −15.40(4H), −16.69(4H), −17.33(4H); m/z (ESMS, ESI^+) 941.14 (100%, $[M+OH_2]^{3+}$), Calcd. 941.37.

Eu(6)—A similar procedure to the synthesis of Eu(**1**) was followed. ^{1}H NMR (400 MHz, CD_3CN) δ 13.4(2H), 7.27(4H), 6.12(4H), 4.79(4H), 4.11(4H), 3.77(6H), 3.63(8H), 3.48(9H), 3.23 to 1.08(8H), −1.2(4H).; m/z (ESMS, ESI^+) 897.482 (100%, $[M+OH_2]^{3+}$) Calcd. 898.33.

Eu(7)—^{1}H NMR (400 MHz, CD_3CN) δ 46.1(2H), 29.4(4H), 13.8(4H), 8.51(3H), 5.07(27H), 3.80(9H), 2.75 to 0.74(8H), −8.24(3H), −8.88(3H), −11.7(4H), −13.8(4H); $MALDI^+$: m/z 935.416 (100%), $[M+H]^+$, Calcd. 936.43.

Eu(8)—^{1}H NMR (400 MHz, CD_3CN) δ 27.9(2H), 16.0(2H), 12.8(2H), 11.51(2H), 9.81(2H), 7.75(2H), 5.23(4H), 4.17(18H), 3.91(18H), 3.36 to −2.03(6H), −4.85(2H), −8.95(2H), −10.29(2H), −11.0(2H), −13.6(2H); $MALDI^+$: m/z 863.611 (100%), $[M+H]^+$, Calcd. 863.42.

Eu(9)—A solution of $EuCl_3$ (9.5 mg, 0.0367 mmol) was added to a solution of **9** (22 mg, 0.0367 mmol) in H_2O (5 mL total). The pH of the solution was maintained between 6 and 7 by the addition of NaOH solution for 24 hours. At the end of this period, the pH was set to 8, and the sample was filtered and freeze-dried to afford the complex as a white solid. ^{1}H NMR (400 MHz, CD_3CN) δ 28.3(2H), 21.65(2H), 18.93(2H), 6.15(2H), 4.62(2H), 4.27(2H), 4.05(3H), 3.97(3H), 3.81(3H), 3.64(2H), 3.47(2H), 3.32(2H), 3.21(2H), 2.82 to −5.07 (8H), −5.54(2H), −7.71(2H), −8.06(2H), −11.0(2H), −12.9(2H); $MALDI^+$: m/z 768.08 (100%), $[M+H]^+$, Calcd 768.24.

Eu(10)—A similar procedure to the synthesis of Eu(**9**) was followed. ^{1}H NMR (400 MHz, CD_3CN) δ 25.8(2H), 17.98(2H), 14.02(2H), 7.95(6H), 4.63(6H), 3.68(6H), 3.25(2H), 3.13(2H), 2.96 to −0.641, −1.48(2H), −8.53(2H), −12.5(2H); $MALDI^+$: m/z 750.944 (100%), $[M+H]^+$, Calcd 751.29.

RESULTS AND DISCUSSION

Our initial hypothesis postulated that cyclen derivatives with simple ketone pendant arms would donate considerably less electron density to a Ln^{3+} ion compared to amide donors and this should result in a significant increase of the metal ion bound water lifetime (see Figure 1). Simple DFT calculation shows that the charge on a C=O oxygen decreases substantially from a carboxylic acid to an amide to a ketone. Since it is now well documented that substituting an amide for a carboxylate donor atom in Ln-polyaminopolycarboxylate complexes substantially increases the bound water residence lifetime,6 the DFT results summarized in Figure 1 predict that substitution of an even weaker ketone donor should produce complexes with even slower water exchange. The calculation does not allow us to predict the magnitude of the effect, however.

The series of chelates chosen to evaluate the variations in water exchange kinetics that might be possible in Eu^{3+}-based PARACEST agents are shown in Chart 2. The impact of ligand donor strength on water exchange kinetics were first explored in the ketone donor ligands **1** and **2**. We subsequently prepared mixed pendant arm ligands derived from DOTA-(gly-tBu)$_4$ (ligand **3**) by sequentially replacing the extended glycinate sidearms with levulonate (ligands **1, 4, 5** and **6**) as well as the bulky pinacolone appendages (ligands **7**–**10**).

Synthesis and characterization of the ligands and their Eu^{3+} complexes

Synthesis of ligands **1**–**3** involved the tetraalkylation of cyclen with the appropriate bromo or chloro derivative of the ketone. Methyl 5-bromolevulinate, required for **1**, was prepared by the bromination of methyl levulinate using a slightly modified literature method.22, 23 Halide precursors used for the synthesis of **2** was commercially available. Ligand **3** first required acylation of the t-Bu protected glycinate arm followed by alkylation of cyclen. Standard alkylation protocols gave the desired ligands **1**–**3** in variable yields (37–75%). Attempted synthesis of the corresponding acid derivatives of **1** and **2** followed by acid hydrolysis resulted in extensive decomposition. Synthesis of the mixed sidearm ligands, **4**–**10**, began with selectively protected cyclen derivatives prepared as previously reported (all synthetic details are provided in supporting information). All ligands were characterized by ^{1}H and ^{13}C NMR spectroscopy, HPLC, MALDI-Mass Spectrometry, and/or elemental analysis (Experimental Section).

The NMR spectrum of **2** provided evidence for keto-enol tautomerism of the side arms, a well-understood phenomenon for β-diketones. Prototropic rearrangements between the keto and the enol forms are acid-base catalyzed and occurs readily in the presence of water. In general, simple ketones exist in the more stable keto form but such compounds can exist in the enol form when stabilized by hydrogen bonding or steric factors.24 A classic example is acetylacetone, a β-dicarbonyl compound in which the enol form is favored due to intramolecular hydrogen bonding. The ^{13}C NMR of **2** showed that the β-dicarbonyl side chains exist predominantly in the enol form as evidenced by the upfield shift of the -carbonyl carbon to about 118 ppm (Scheme 1). In contrast, the absence of peaks around 120 ppm in the ^{13}C NMR of ligand **1** (Supplemental Information) suggests that this γ-dicarbonyl derivative exists primarily in the keto form, consistent with the fact that intramolecular stabilization of the enol form by H-bonding does not occur in γ-dicarbonyl compounds (Figures S1 and S2).24 Ligand **11**, shown in Chart 3, was designed to prevent keto-enol tautomerization via gem-dimethyl substitution on the carbon to the ketone carbonyl. As expected, enol species were not observed in the ^{13}C spectrum of **11** (Figure S3). NMR spectra of the remaining diketone ligands in Chart 2 (**4**, **5** & **6**) showed no evidence for enol formation.

The Eu^{3+} complexes of **1–10** were prepared from the corresponding ligands by addition of either europium triflate in acetonitrile or europium chloride in water. The complexation reactions were run up to 3 days due to the slow formation kinetics of DOTA-like complexes. 6 The complexes were characterized by MALDI-mass spectrometry and ^{1}H NMR. Although several routes were attempted, we were unable to obtain a Eu^{3+} complex of **11** likely due to the increased steric bulk of the gem-dimethyl groups. The ^{1}H NMR spectra of Eu(**1**) and Eu(**2**) were recorded in CD_3CN. A notable feature of these spectra is that the observed Eu^{3+} induced ^{1}H hyperfine shifts are significantly smaller than those of other Eu^{3+} DOTA-like complexes consistent with the anticipated weaker ligand field provided by the ketone donor groups. In both cases, a resonance observed near 15 ppm that disappeared upon addition of 10 μL aliquots of D_2O to the sample was tentatively assigned to a Eu^{3+}-bound water species. Similarly, resonances with similar exchange characteristics were seen in ^{1}H NMR spectra of Eu(**4**) (46 ppm), Eu(**5**) (35 ppm) and Eu(**6**) (15 ppm). This trend is consistent with sequential substitution of amide side-arms with ketone side-chain donors (the Eu^{3+}-bound water resonance is near 50 ppm in most DOTA-tetraamide complexes). Closer inspection of the high resolution ^{1}H NMR spectrum of Eu(**5**) showed that two coordination isomers were present in solution. 2D-EXSY spectroscopy of this complex showed interconverting species, consistent with square anti-prism (SAP) and twisted square antiprism (TSAP) coordination isomers (Figure S3).6, 25 Given that water exchange in TSAP isomers is generally about two orders of magnitude faster than in SAP isomers and, consequently, the Eu^{3+}-bound water resonance in the TSAP isomer is typically not detected by ^{1}H NMR near room

temperatures,6 the exchangeable peaks observed here for Eu(**5**) is most logically assigned to the SAP isomer. Similarly, the exchangeable proton resonance seen in the NMR spectra of Eu(**1**), Eu(**2**), Eu(**4**) and Eu(**6**) likely also reflects SAP isomers in these complexes.

A proton exchangable resonance (presumably Eu-OH_2) was also observed in ^{1}H NMR spectra of Eu(**7**), Eu(**8**), Eu(**9**) and Eu(**10**) in CD_3CN. All resonances in the spectra of Eu(**7**) and Eu(**8**) were quite broad compared to the others, consistent more dynamic, less rigid structures. Again, sequential replacement of amide side-arms with the more bulky t-butyl ketone arms resulted in an upfield shift in the Eu-OH_2 resonances, consistent with earlier series. 2D-EXSY NMR of Eu(**8**) also indicated the presence of two interchanging isomers. Interestingly, the exchangeable Eu-OH_2 resonances in Eu(**9**) and Eu(**10**) appear at 29 and 26 ppm, respectively, much less differentiated on the basis of chemical shift than the corresponding exchangeable Eu-OH_2 resonances in the esters, Eu(**7**) and Eu(**8**). This indicates that the ligand field created by the ligand side-arms is somewhat stronger in the ester versus the free acid complexes. Nonetheless, the general trend in Eu^{3+}-bound water chemical shifts with ketone substitution, albeit less pronounced, remains intact for this series of chelates as well. The observation that the Eu-OH_2 proton resonance in Eu(**9**) appears further upfield than the corresponding Eu-OH_2 proton resonances in other mono-substituted ketone derivatives (Eu(**4**) and Eu(**7**)) suggests that the greater negative charge in Eu(**9**) contributes to a weaker ligand field.

The relationship between the position of the Eu-OH_2 resonance and the macrocycle H_4 protons is another notable feature for this series of mixed donor ligands. For other EuDOTA-tetraamide based systems, the H_4 resonance is consistently observed at a chemical shift about 50% that of the Eu-OH_2 resonance (determined by the geometry of the complex, see for example the data point for Eu(**3**) in Fig. 2).6 This relationship differs somewhat for the mixed ketone/amide systems (Figure 2). For chelates containing 3 amides and 1 ketone side-arms (Eu(**4**) and Eu(**7**)) the chemical shifts of H_4 protons are ~66% of the chemical shifts of the Eu-OH_2 resonances. For ligands containing 2 amide and 1 ketone side-arms (Eu(**5**) and Eu(**8**)), the chemical shift of the H_4 protons are ~60% of the chemical shift of the respective Eu-OH_2 resonances. The acid derivatives (Eu(**9**) and Eu(**10**)) follow a similar trend. The fact that this ratio changes with side-arm substitution indicates that the geometry of the H_4 proton relative to the Eu-bound water protons differs somewhat in these complexes. If one assumes that the Eu-N bonds remain relatively constant among this series, then the larger hyperfine shift of H_4 relative to Eu-OH_2 can be explained entirely by lengthening of the Eu-water oxygen bond distance as amides are replaced by ketone side-chains. The absolute chemical shift of the H_4 protons can serve as a spectroscopic handle for the strength of the ligand field, with strong field ligands producing larger, downfield shifts. Based on the experimental observations then, substitution of an amide donor by a ketone donor clearly produces a weaker ligand field throughout this series.

CEST spectra and metal bound water residence lifetimes

CEST spectroscopy was used to determine the bound water lifetimes (τ_m) in each complex where a CEST exchange peak from the Eu^{3+}-bound water molecule was observed (Figures S4–S11). CEST spectra were collected in either a 1:1 mixture of water and acetonitrile, or in pure water for the water soluble acid derivatives, Eu(**9**) and Eu(**10**). The measured bound water lifetimes and the position of the Eu^{3+}-bound water exchange peak are compiled in Table 1. The bound water lifetimes increased from 345 to 395 to 475 μs along the series Eu(**3**), Eu(**4**) and Eu(**5**), supporting our hypothesis that an increase in the number of ketone donors does indeed slow water exchange (longer τ_m). A similar increase in τ_m was observed from Eu(**9**) to Eu(**10**) but, interestingly, this was not observed for the corresponding esters, Eu(**7**) to Eu(**8**). The unexpectedly short τ_m value of Eu(**8**) is due to the fact that this complex has a lower SAP/TSAP ratio than Eu(**7**) (see later discussion).

For most complexes, a Eu^{3+}-bound water exchange peak was observed at or near the same chemical shift as the described above for the exchangeable bound water resonance as observed by high resolution ^1H NMR (spectra recorded in CD_3CN). This suggests there may be some differences in the structures of some complexes in CD_3CN as solvent *versus* 50:50 water:acetonitrile as solvent. For example, the high resolution ^1H spectra of Eu(**4**) and Eu(**5**) collected in nearly dry CD_3CN show D_2O exchangeable water peaks at 46 and 35 ppm, respectively, whereas the CEST spectra collected in 50:50 water:acetonitrile show exchangeable water peaks at 34 and 26 ppm, respectively (Figure 3). This suggests a chemical rearrangement occurs with the complex in water that results in a somewhat weaker ligand field experienced by the Eu^{3+}, reflected by the ~25% smaller hyperfine shifts. Closer examination of the CEST spectra of Eu(**4**) and Eu(**5**), reveal that in addition to the Eu^{3+}-bound water exchange peaks at 34 and 26 ppm, respectively, other exchanging peaks are present in these spectra near 5 and 3 ppm, respectively. Since these ligand side arms could in principle rearrange to the enol form in the presence of water (with the enol −OH acting as the ligand donor to the Eu^{3+} ion), the peaks at 5 and 3 ppm could possibly reflect either Eu^{3+}-bound −OH exchange peaks resulting from enol rearrangement or to a Eu^{3+}-bound water molecule in the enol form of the complex. With either assignment, the observation that the Eu^{3+}-bound water exchange peaks observed at 46 or 35 ppm (for Eu(**4**) and Eu(**5**), respectively) in neat acetonitrile shift to 34 and 26 ppm, respectively, in 50:50 water:acetonitrile indicates that the enol form (−OH) provides a weaker ligand field than does the keto form. These putative −OH exchange peaks have similar chemical shifts as observed previously for −OH exchange peaks in $EuCNPHC^{3+}$, a complex having a single amide side-chain plus three hydroxyethyl side-chains (Chart S1 in SI).12 A previous report on this complex established that the hydroxyl groups remain protonated (and hence show exchange peaks in the CEST spectra) in predominantly acetonitrile solutions but disappear upon addition of excess water. Similarly, the CEST exchange peaks observed here for Eu(**4**) and Eu(**5**) disappear entirely when dissolved in 80:20 water:acetonitrile. This provides further evidence for the assignment of the small exchange peaks near 5 and 3 ppm in CEST spectra of Eu(**4**) and Eu(**5**) to exchanging enol −OH protons. The absence of enol −OH exchange peaks in CEST spectra of Eu(**7**–**10**) is also consistent with this assignment (Figure 4).

Interestingly, the CEST spectra of those complexes containing three or more ketone side-arms, Eu(**1**), Eu(**2**) and Eu(**6**) did not show a Eu^{3+}-bound water exchange peak in 50:50 H_2O:CH_3CN at room temperature. CEST spectra for these same complexes run in nearly dry CH_3CN did show a small CEST exchange peak near 4 ppm, again consistent with either enol −OH exchange peaks or a weakly shifted Eu^{3+}-bound water exchange peak.

Figure 4 compares CEST spectra of Eu(**7**) and Eu(**8**) in H_2O:CH_3CN. The exchange peaks at 38 and 26 ppm, respectively, are easily assigned to Eu^{3+}-bound water exchange peaks based upon comparisons to their high resolution NMR spectra. As expected, ligand **8**, with two ketone donor groups, produces a weaker ligand field for Eu^{3+} than does ligand **7** with only one ketone donor. This is manifested by the smaller $\Delta\omega$ for the water exchange peak in Eu(**8**). However, the smaller $\Delta\omega$ in this case does not translate to a longer bound water lifetime since Eu(**7**) displays slower water exchange (τ_m= 310 μs) than Eu(**8**) (τ_m = 185 μs) so other factors must come into play here. One possibility is the presence of SAP versus TSAP isomers in these complexes. The ^1H NMR spectrum of Eu(**7**) shows that this complex exists in solution largely as the SAP isomer while the spectrum of Eu(**8**) shows two coordination isomers. 2D-EXSY spectroscopy of Eu(**8**) shows that these are interconverting SAP/TSAP species (data not shown) with the TSAP predominating (40% SAP, 60% TSAP). The CEST spectrum of Eu(**8**) also shows only a small Eu^{3+}-bound water exchange peak at 27 ppm, consistent with a small population of the SAP isomer in this sample. Given that water exchange in the predominant TSAP isomer is expected to be too fast to be observed

by CEST in this species, its presence however will affect the measured residence water lifetime in samples consisting of lesser quantities of the SAP isomer.6 This is the likely reason why τ_m for Eu(**8**) is much smaller (185 μs) than what one might have anticipated based on its chemical structure.

The greater proportion of TSAP isomer found in Eu(**8**) likely reflects increased steric encumbrance around the Eu^{3+} ion imposed by the two bulky ketone side-arms placed in close proximity to the bulky tert-butyl groups on the glycinate arms. Removal of the tert-butyl ester groups had only a small impact on water exchange in complexes containing one ketone side-arm (compare τ_m in Eu(**7**) (310 μs) and Eu(**9**) 332 μs) but had a dramatic effect in complexes containing two ketone side-arms (compare τ_m in Eu(**8**) (185 μs) and Eu(**10**) 416 μs). Unlike Eu(**8**), Eu(**10**) exists largely as a SAP isomer in solution (>90%) so removal of the bulky tert-butyl ester groups has a rather dramatic effect on overall structure and on water exchange kinetics in this system. It is also interesting to note that the intensity of the Eu^{3+}-bound water exchange peaks in Eu(**9**) and Eu(**10**) were sensitive to changes in pH, showing an optimal CEST intensities at pH = 6.4 and diminishing CEST with further increases in solution pH (Figure S12). This may in part reflect the effects of pH on acid/base catalyzed keto-enol isomerization.

CONCLUSIONS

A series of cyclen based ligands with ketone sidearms were synthesized and PARACEST properties of the corresponding Eu^{3+} complexes examined. Ligands **1**, **2** and **11** containing only ketone sidearms established that keto-enol isomerization plays a role in structural make-up of this class of chelates and suggested that the ketone groups may prefer to bind with the metal ion in the enolate form. For Eu^{3+} complexes containing mixed donor (amide/ketone) side-chains, ligands **4**–**10**, each amide to ketone substitution resulted in slower water exchange and smaller Δω, consistent with our hypothesis that weak field ligands will yield complexes with slower water exchange kinetics by placing more positive character on the central lanthanide ion. Other features including coordination geometry (Eu(**8**)) and steric hindrance (likely a component in Eu(**7–10**)) clearly influence water exchange and the resulting PARACEST properties. Although solvent compatibility will likely hinder the use of many of these systems to vitro applications only, this work lays the foundation for the design of other, weak donor systems capable of producing slower water exchange.

Supplementary Material

Refer to Web version on PubMed Central for supplementary material.

Acknowledgments

Financial support from the National Institutes of Health (CA115531, RR02584, and EB004582) and the Robert A. Welch Foundation (AT-584) is gratefully acknowledged. We gratefully acknowledge the Johann Deisenhofer laboratory for use of their computational equipment and programs.

References

1. Caravan P, Ellison JJ, McMurry TJ, Lauffer RB. Chem. Rev. 1999; 99:2293. [PubMed: 11749483]
2. Yoo B, Pagel MD. Front. Biosci. 2008; 13:1733. [PubMed: 17981664]
3. Woods M, Zhang S, Sherry AD. Curr. Med. Chem.: Immunol., Endocr. Metab. Agents. 2004; 4:349. [PubMed: 20686642]
4. Merbach, AE.; Toth, E. The Chemistry of Contrast Agents in Medical Magnetic Resonance Imaging. Chichester, UK: Wiley; 2001.
5. Major JL, Meade TJ. Acc. Chem. Res. 2009; 42:893. [PubMed: 19537782]

6. Viswanathan S, Kovacs Z, Ratnakar J, Green KN, Sherry AD. Chem. Rev. 2010; 110:2960. [PubMed: 20397688]
7. Ward KM, Aletras AH, Balaban RS. J. Magn. Reson. 2000; 143:79. [PubMed: 10698648]
8. Micskei K, Helm L, Brucher E, Merbach AE. Inorg. Chem. 1993; 32:3844.
9. Dunand FA, Borel A, Helm L. Inorg. Chem. Commun. 2002; 5:811.
10. Zhang S, Jiang X, Sherry AD. Helv. Chim. Acta. 2005; 88:923.
11. Viswanathan S, Ratnakar SJ, Green KN, Kovacs Z, De Leon-Rodriguez LM, Sherry AD. Angew. Chem., Int. Ed. 2009; 48:9330.
12. Woods M, Woessner DE, Zhao P, Pasha A, Yang M-Y, Huang C-H, Vasalitiy O, Morrow JR, Sherry AD. J. Am. Chem. Soc. 2006; 128:10155. [PubMed: 16881645]
13. Lee J, Brewer M, Berardini M, Brennan JG. Inorg. Chem. 1995; 34:3215.
14. Bunzli, JC.; Choppin, GR. Lanthanide Probe in Life, Medical and Environmental Science. Amsterdam: Elsevier; 1989.
15. Huang, CH. Rare Earth Coordination Chemistry: Fundamentals and Applications. Singapore: Wiley; 2010.
16. Woessner DE, Zhang S, Merritt ME, Sherry AD. Magn. Reson. Med. 2005; 53:790–799. [PubMed: 15799055]
17. Krogh-Jespersen K, Romanelli MD, Melman JH, Emge TJ, Brennan JG. Inorganic Chemistry. 2010; 49:552. [PubMed: 20025288]
18. Frisch, MJT.; Trucks, GW.; Schlegel, HB.; Scuseria, GE.; Robb, MA.; Cheeseman, JR.; Montgomery, JA., Jr; Vreven, T.; Kudin, KN.; Burant, JC.; Millam, JM.; Iyengar, SS.; Tomasi, J.; Barone, V.; Mennucci, B.; Cossi, M.; Scalmani, G.; Rega, N.; Petersson, GA.; Nakatsuji, H.; Hada, M.; Ehara, M.; Toyota, K.; Fukuda, R.; Hasegawa, J.; Ishida, M.; Nakajima, T.; Honda, Y.; Kitao, O.; Nakai, H.; Klene, M.; Li, X.; Knox, JE.; Hratchian, HP.; Cross, JB.; Bakken, V.; Adamo, C.; Jaramillo, J.; Gomperts, R.; Stratmann, RE.; Yazyev, O.; Austin, AJ.; Cammi, R.; Pomelli, C.; Ochterski, JW.; Ayala, PY.; Morokuma, K.; Voth, GA.; Salvador, P.; Dannenberg, JJ.; Zakrzewski, VG.; Dapprich, S.; Daniels, AD.; Strain, MC.; Farkas, O.; Malick, DK.; Rabuck, AD.; Raghavachari, K.; Foresman, JB.; Ortiz, JV.; Cui, Q.; Baboul, AG.; Clifford, S.; Cioslowski, J.; Stefanov, BB.; Liu, G.; Liashenko, A.; Piskorz, P.; Komaromi, I.; Martin, RL.; Fox, DJ.; Keith, T.; Al-Laham, MA.; Peng, CY.; Nanayakkara, A.; Challacombe, M.; Gill, PMW.; Johnson, B.; Chen, W.; Wong, MW.; Gonzalez, C.; Pople, JA. Gaussian 03. Wallingford, CT: Gaussian, Inc.; 2004. revision D.01
19. Dickson RM, Becke AD. J. Chem. Phys. 1993; 99:3898.
20. Lee C, Yang W, Parr RG. Physical Review B: Condensed Matter and Materials Physics. 1988; 37:785.
21. GaussView, VG. Version 4.1. Dennington, R., II; Keith, T.; Millam, J., editors. Shawnee Mission, KS: Semichem, Inc.; 2007.
22. Sorg A, Siegel K, Brueckner R. Chem.--Eur. J. 2005; 11:1610.
23. Zhang Y, Wu L, Li F, Li B-G. Synthetic Communications. 2005; 35:2729.
24. Kemp, DS.; Vellaccio, F. Organic Chemistry. New York: Worth Publishers; 1980.
25. Vipond J, Woods M, Zhao P, Tircso G, Ren J, Bott SG, Ogrin D, Kiefer GE, Kovacs Z, Sherry AD. Inorg. Chem. 2007; 46:2584. [PubMed: 17295475]

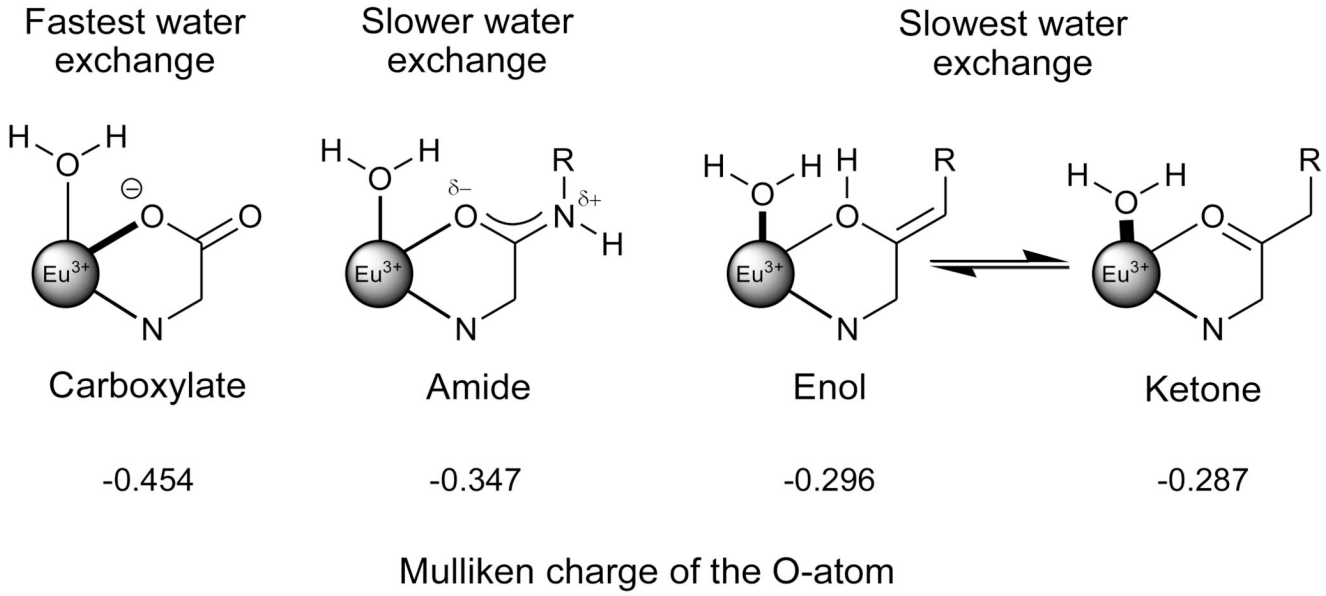

Figure 1.
Expected resonance contributions in europium (III) chelate bonds in ligands containing a carboxylate oxygen, an amide oxygen, enol oxygen or a ketone oxygen donor and the anticipated trends in the metal-bound water oxygen bond lengths and bound water residence lifetimes. The calculated Mulliken charges on the oxygen donor atom in each type of complex is also shown.

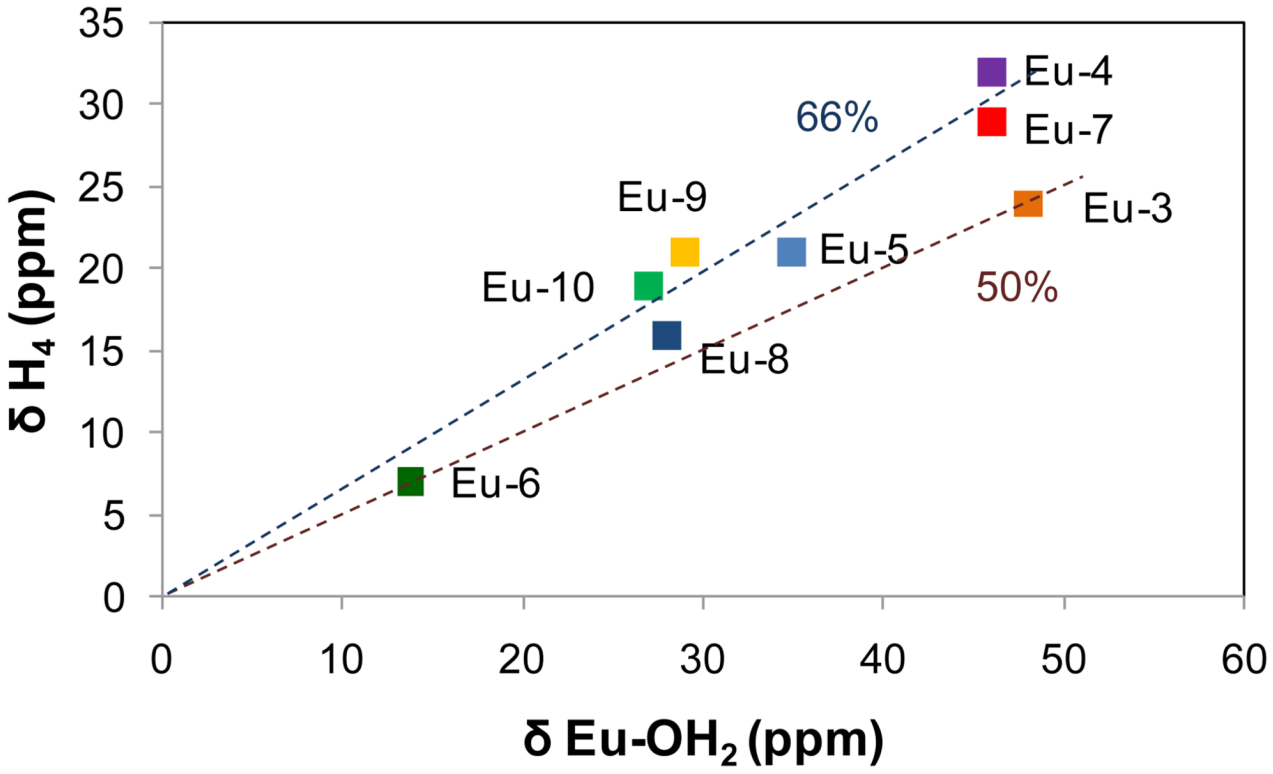

Figure 2.
Comparison of chemical shifts of the Eu-OH_2 resonances vs. the H_4 ligand proton resonances in each complex (measured in CD_3CN). The two dashed lines correspond to 66 % and 50 % of the δH_4 / δEu-OH_2 ratios, respectively.

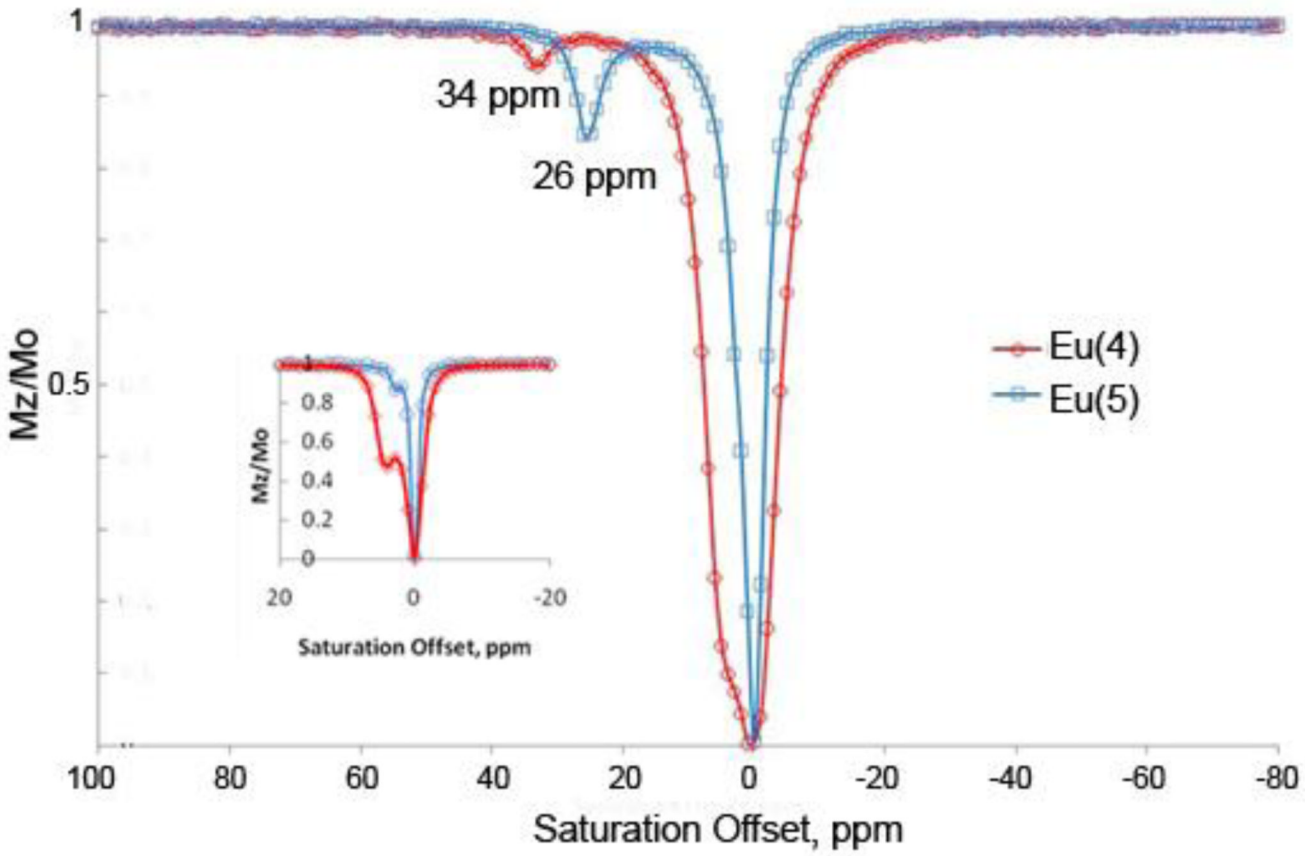

Figure 3.

CEST spectra of Eu(**4**) (red) and Eu(**5**) (blue) recorded at 9.4 T and 298 K in CH_3CN at B_1 = 10.8 μT (459Hz) and 10.0 μT (426 Hz), respectively. (Inset: B_1= 2.5 μT for both spectra.)

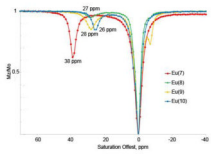

Figure 4.

The CEST spectra of Eu(**7**) (red, 17 mM), Eu(**8**) (green, 30 mM total, 12 mM SAP), Eu(**9**) (yellow, 18 mM) and Eu(**10**) (blue, 3.6 mM) recorded at 400 MHz and 298K in H_2O:CH_3CN (1:1) for Eu(**7**) and Eu(**8**) and water for Eu(**9**) and Eu(**10**) using applied B_1 field of 10.4 μT.

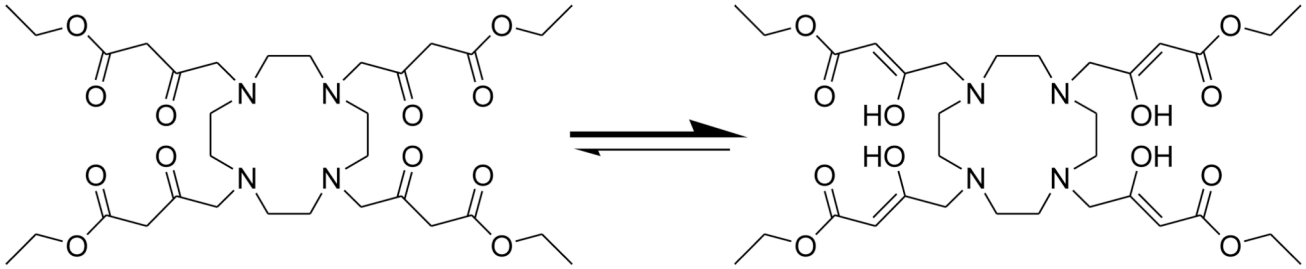

Scheme 1.
Keto-enol tautomerism in ligand **2**.

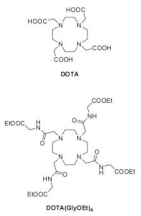

Chart 1.

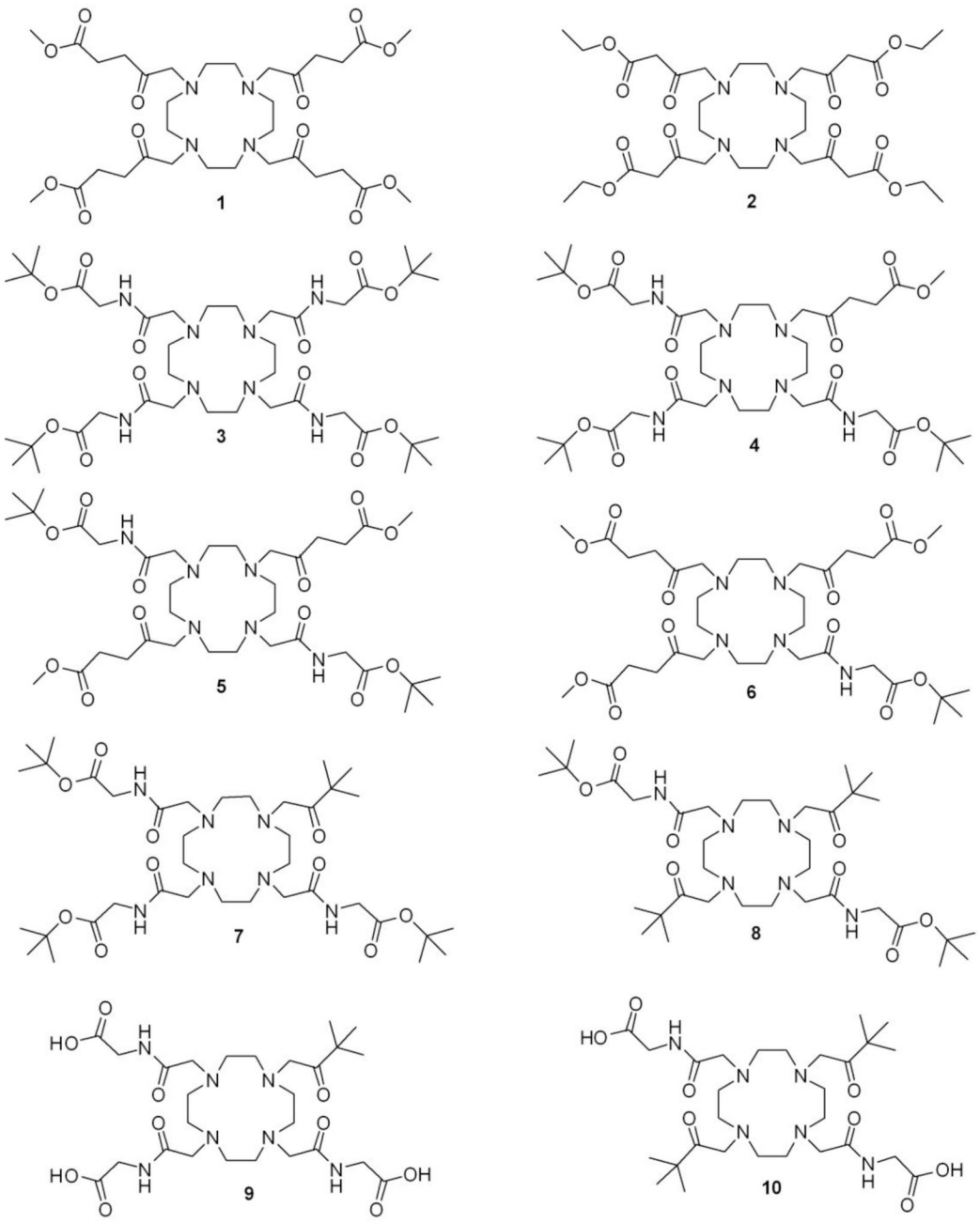

Chart 2.

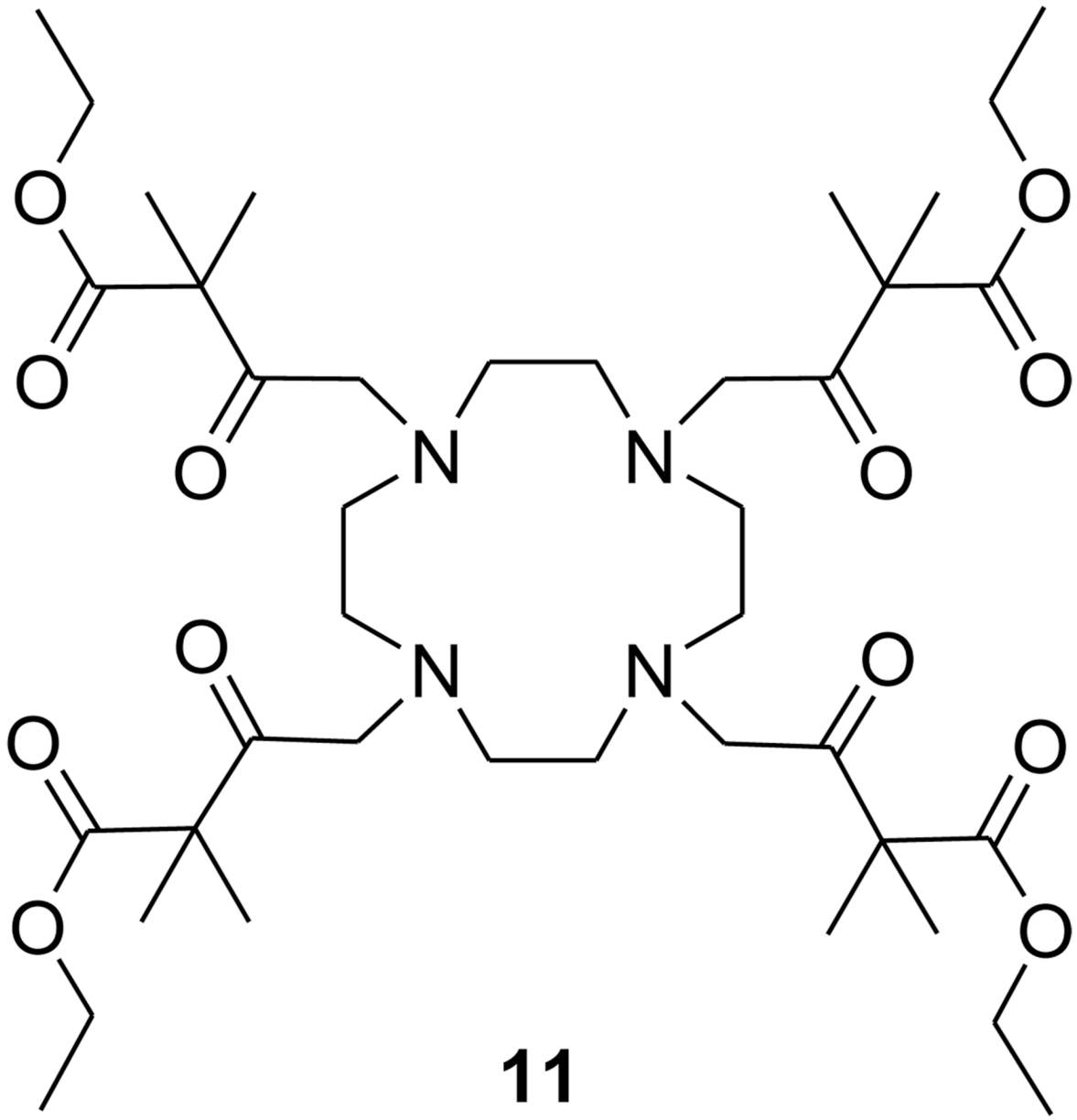

11

Chart 3.

Table 1

Chemical shift of CEST exchange peaks and the bound water lifetimes for Eu^{3+} complexes examined in this study.

	δ Eu-OH_2 (ppm)	τ_m (μs)[a]	Solvent
Eu(**3**)	48	345±12	H_2O/CH_3CN[b]
Eu(**4**)	34	395	H_2O/CH_3CN[b]
Eu(**5**)	26	475	H_2O/CH_3CN[b]
Eu(**7**)	38	310±5	H_2O/CH_3CN[b]
Eu(**8**)	26	185±3	H_2O/CH_3CN[b]
Eu(**9**)	28	332±5	H_2O
Eu(**10**)	27	416±12	H_2O

[a] The τ_m values were obtained by fitting the CEST data obtained at different B_1 values to the Bloch equations.16 The ± values represent the error in multiple fittings.

[b] The ratio of H_2O/CH_3CN was 1:1.